



GREEN SYNTHESIS OF ZINC OXIDE NANOPARTICLES USING *SOLANUM NIGRUM* LEAF EXTRACT AND OVERVIEW OF THEIR ANTIBACTERIAL ACTIVITIES

Helen Merina Albert*¹, C. Alosious Gonsago²

¹Department of Physics, Sathyabama Institute of Science and Technology, Chennai, India

²Department of Electronics Science, Mohamed Sathak College of Arts and Science, India

*Corresponding author: drhelenphy@gmail.com

Received: 03-04-2023; Accepted: 05-05-2023; Published: 31-05-2023

© Creative Commons Attribution-NonCommercial-NoDerivatives 4.0 International License <https://doi.org/10.55218/JASR.202314505>

ABSTRACT

In the current study, we have described the green synthesis of ZnO nanoparticles (ZnO-NPs) employing the capping ingredient *Solanum Nigrum*. With the use of X-ray diffraction (XRD), Fourier transform infrared (FT-IR) spectroscopy, UV-Vis absorption, and antibacterial investigations, the functionalization of ZnO particles through *Solanum Nigrum* leaves extract-induced bio-reduction of ZnO was examined. According to XRD analysis, the produced NPs have a wurtzite hexagonal structure and have an average grain size of 27.6 nm. The functional groups are further shown by FT-IR spectra. The band gap is estimated to be 3.38 eV based on UV-Vis DRS studies. It has been proven that the particle size variations and surface area-to-volume ratios of ZnO-NPs are responsible for significant higher antibacterial activities. According to the antibacterial study, the ZnO-NPs inhibit the growth of both normal as well as pathogenic bacterium and hence might be used for coating surgical equipments for performing aseptic operators in the medical field.

Keywords: Green synthesis, *Solanum Nigrum* Leaf, XRD, FTIR, Antibacterial study.

1. INTRODUCTION

Nanotechnology deals with the creation of materials, devices and systems within the nanometer scale (1-100 nm) through manipulating matter at that scale and exploiting novel properties arising due to the nanoscale. Nanomaterials usually have very different properties from their bulk counterparts, thanks to the importance of quantum and surface boundary effects. The principal parameters of nanoparticles are their shape, size, surface characteristics and inner structure. Due to their smaller size, nanoparticles exhibit a wide range of physical or chemical characteristics, such as colloidal qualities, optical, or electric characteristics [1-3]. Nanoparticles (NPs) have become increasingly important in research and development and have a wide range of potential applications in the fabrication of electronic, optoelectronic, LEDs, storage systems, chemical and biological sensors, fibre-optic systems, magneto-optic systems, and optical devices. Recent research [4-8] demonstrates the importance of environmentally friendly methods for creating metal oxide nanoparticles, where oxides of metals including zinc, gold, copper, silver, and nickel are becoming more significant. However, ZnO-

NPs stand out among the different metal oxides due to their strong electron mobility, significant exciton binding energy, wide bandgap, and good optical transmittance [9, 10]. The fabrication of sensors makes use of the optical characteristics of zinc oxide [11, 12]. In the current study, ZnO-NPs are made via a green synthesis process using the leaves of *Solanum Nigrum* plant.

Natural substances play a crucial and multifaceted role in the synthesis of nanoparticles and serve as capping agents to solidify them are found in biological systems. According to the literature review, plants have significant benefits over other biological systems. The plants are readily accessible, secure to handle, and yield more stable nanoparticles than other methods [13-15]. In moist environments, *Solanum Nigrum* (Solanaceae), also known as Makoi or poisonberry, typically develops as a weed in a variety of soil types, including dry, stony, shallow, or deep soils. It may also be grown in tropical and subtropical agro-climatic regions. *Solanum Nigrum* leaf is medicinally employed in the management of several ailments, like pneumonia aching teeth, stomach ache, tonsillitis, wing worms, pain, inflammation, fever, tumour, as a tonic, as an antioxidant, anti-inflammatory,

as hepatoprotective, as diuretic, and as antipyretic. The *Solanum Nigrum* plant is usually used as an elemental ingredient for clinical traditional Chinese medicine cancer therapy. Using the *Solanum Nigrum* leaf extraction technique and Zinc Chloride as a chemical building block, ZnO-NPs are synthesized. The produced samples are further distinguished by X-ray diffraction, UV-spectroscopy, FTIR, and antibacterial activity.

The process of eradicating or inhibiting disease-causing germs is referred to as antibacterial activity. For this, a variety of antibacterial agents are used. The main justification for considering NPs as an alternative to antibiotics is that in some circumstances, NPs can effectively inhibit microbial drug resistance [16-18]. The rampant use of antibiotics has led to the emergence of various hazards to public health, like superbugs that don't answer any existing drug and epidemics against which medicine has no defence. The look for new, effective bactericidal materials is important for combating drug resistance, and NPs are established as a promising approach to resolve this problem. In the present study, we present the positive and negative aspects of the interactions between NPs and drug-resistant bacteria. The Green synthesized ZnO-NPs inhibit the growth of both normal as well as pathogenic bacterium and hence

might be used for coating surgical equipments for aseptic operators in the medical field.

2. EXPERIMENTAL

Fresh leaves of *Solanum Nigrum* plant were collected from Chidambaram, Tamil Nadu, India. To get rid of the dust, the leaves were rinsed many times with distilled water. In order to make the extract, 100g of washed; dried leaves were combined with 500ml of distilled water in a beaker. The mixture was boiled for 20 minutes, until the colour changed from watery to light yellow, after which the extract was cooled to room temperature and filtered through Whatman filter paper. Then the extract was stored at room temperature. The fresh leaves of *Solanum Nigrum* and their extract are shown in Fig. 1.

To synthesize ZnO-NPs, 100 ml of *Solanum Nigrum* leaf extract was heated using a stirrer heater. When the temperature reached 60°C, 10g of Zinc Chloride was added to the solution. Afterward, this combination was heated until it turned into a deep yellow suspension. The paste was then gathered in a ceramic crucible and centrifuged at 10,000 rpm for 10 minutes. A light white powder was produced, which was carefully collected. Using a mortar and pestle, the substance was ground into a fine powder and used for various characterizations.



Fig. 1: (a) *Solanum Nigrum* leaves, and (b) Extract of *Solanum Nigrum* leaves.

3. RESULTS AND DISCUSSION

3.1. Powder X-ray Analysis

Powder X-ray diffraction (XRD) analysis is a convenient analytical method that mainly determines the phase of a crystalline material and can give details about the dimensions of unit cells [19, 20]. The substance under analysis is finely ground, blended, and the bulk composition is calculated on average. $\text{CuK}\alpha$ radiation

with a wavelength of 1.541 Å was used to generate the diffraction patterns. A tiny amount of the sample was placed on a glass plate for XRD analysis. The scanning was carried out in the 2θ range from 20° to 80° at a rate of 0.02 min^{-1} . The device was run at a current of 30 mA and a voltage of 40 kV.

The diffraction patterns of ZnO-NPs are depicted in Fig. 2. The diffraction peaks appeared at 2θ value of 31.62°,

34.38°, 36.34°, 47.58°, 57.12°, 63.75°, and 69.24°. These peaks, in order, correlate to the planes (100), (002), (101), (102), (110), (103), and (112), indicate the crystal structure of the particles. The planes exhibit good agreement with the JCPDS file (JCPDS card no. 80-0075). Furthermore, XRD analysis also shows that all the diffraction peaks fit well with the hexagonal wurtzite structure of ZnO-NPs. The average crystal size of the green synthesized Zn-NPs has been determined from the three most intense peaks using Debye–Scherrer’s equation [21, 22]:

$$D = \frac{0.89\lambda}{\beta \cos\theta} \text{ nm}$$

Where D is the average crystalline size (nm), λ is the Cu-K α radiation wavelength (Å), β is the full-width at half-maximum (radian) and θ is the scattering angle (degree). The average particle size of produced ZnO-NPs was determined to be 27.6 nm using the above equation.

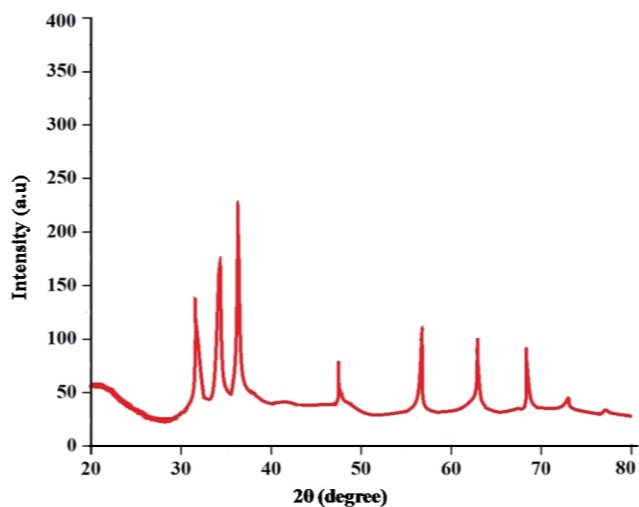


Fig. 2: XRD diffraction patterns of green synthesized ZnO-NPs

3.2. FT-IR Analysis

FT-IR is an analytical technique used to obtain an infrared spectrum of absorption or emission of a solid, liquid or gas [23]. The functional groups got involved to ZnO-NPs were identified in the 4000-400 nm region. The samples were made by evenly dispersing ZnO-NPs in a matrix of dry KBr, which was eventually compressed to yield a transparent disc. KBr pellets were used as a reference. The observed FT-IR spectra of ZnO-NPs is shown in Fig. 3. The absorption bands at 3429, 2926, 2349, 1635, 1404, 1261, 1031, 605, 540, and

470 cm^{-1} in *S. Nigrum* leaf extract would be shifted into 3425, 2924, 1627, 1382, 1126, 1030, 833, and 445 cm^{-1} in the synthesized ZnO-NPs sample. The peaks found at around 1450-1500 cm^{-1} show the stretching of N-H vibration. The stretching of ZnO-NPs were found around 400-800 cm^{-1} . The FT-IR spectra show the presence of bonds due to O-H stretching around 3429 cm^{-1} and CH-stretching around 2924 cm^{-1} , respectively. The peak at 1404 cm^{-1} may be assigned to the symmetric stretching of the carboxyl side groups in the amino acid residues of the protein molecules. The FT-IR analysis shows that the carbonyl groups in amino acid residues and proteins have a higher affinity for binding metal ions, suggesting that proteins may contain metal nanoparticles.

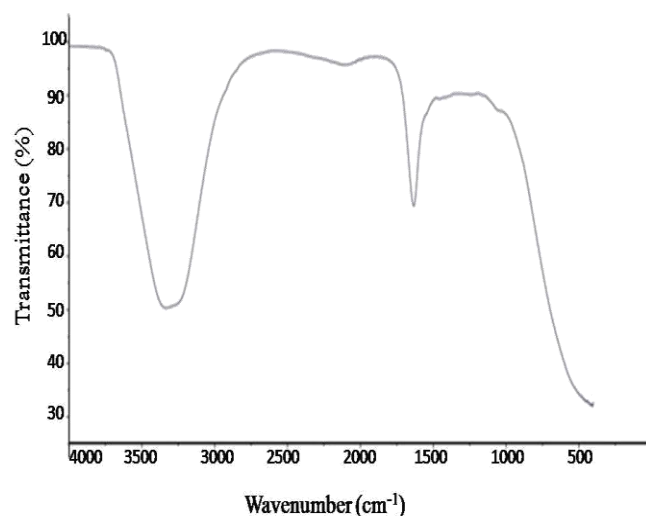


Fig. 3: FT-IR spectra of green synthesized ZnO-NPs.

3.3. UV- Visible spectroscopy

The confirmation of the formation of ZnO-NPs was performed by the UV-Vis spectroscopic analysis. The UV-Vis reflectance spectra (UV-Vis DRS) were carried out using PAN analytical X’PERT PRO instrument operating at a voltage of 50 kV and a current of 30mA in the wavelength range of 200-850 nm at a scan rate of 200nm/min in the reflectance mode. The optical absorption spectrum of ZnO-NPs synthesized with *S. Nigrum* leaf extract is shown in Fig. 4. The sample has a clear and strongly observed absorption below at 400 nm. The optical absorption is minimal from 325nm to 700nm range. The bandgap energy (E_g) of ZnO-NPs was obtained from the absorption limit and can be roughly evaluated by the following relation:

$$E_g = \frac{1240}{\lambda} \text{ eV}$$

Where, E_g is the band gap energy (eV), and λ is the wavelength corresponding to lower absorption limit (nm). The absorption edge at 342 nm corresponds to a bandgap value of 3.63 eV, indicating a red shift in the UV region.

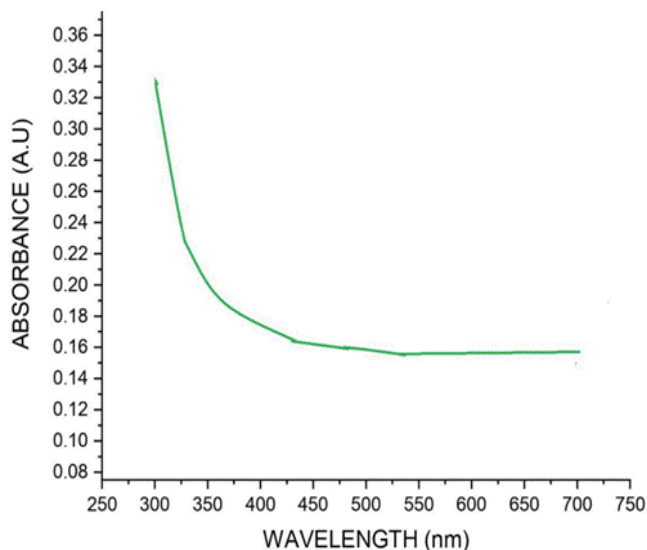


Fig. 4: UV-Vis absorption spectrum of green synthesized ZnO-NPs.

3.4. Antibacterial Activity

ZnO-NPs have become an efficient antibacterial against bacteria that are multidrug-resistant due to their high surface-to-volume ratio and unique physiochemical properties [24, 25]. The antibacterial ability of green

synthesized ZnO-NPs against two bacterial species, *Escherichia coli* and *Salmonella typhi*, was examined in this study using Mueller-Hinton agar plates. Briefly, sterile agar medium was poured in a sterile petridish aseptically and allowed for solidification for 30 minutes. Overnight bacterial culture was inoculated in the medium, and ZnO-NPs were loaded in the well and the dishes were incubated with 37°C about 24 h in bacterial incubator. Just following the incubation time, the zone of inhibition was identified surrounding the well. Antibacterial ability of the green synthesized ZnO-NPs had been observed by determining the diameter of the zone of inhabitation. Antibacterial ability of the green synthesized ZnO-NPs had been tested for three distinct concentrations 20, 40 and 60 μ l. Antibacterial activity was observed in the plate treated with ZnO nanoparticles. Clear zone of inhibition was noted in *E.coli* and *S.typhi* plates at all the concentrations viz 20, 40, and 60 μ l respectively. Notably, *E.coli* is highly susceptible for ZnO nanoparticles compared to *S.typhi*. Based on the results *E.coli* has 6, 8 and 10 mm zone of inhibitions for 20, 40, and 60 μ l concentrations of ZnO nanoparticles respectively. However *S.Typhi* has 3, 5 and 8 mm zone of inhibitions for 20ul, 40ul, 60ul concentrations of ZnO nanoparticles respectively. The zone of inhibition for the *E.coli* and *S.typhi* bacterial species of green synthesized ZnO-Nps are depicted in Fig. 5. According to the obtained results, the ZnO nanoparticles inhibit the growth of both normal as well as pathogenic bacterium. Also, it has been observed that the antibacterial activity increases by increasing the concentration.

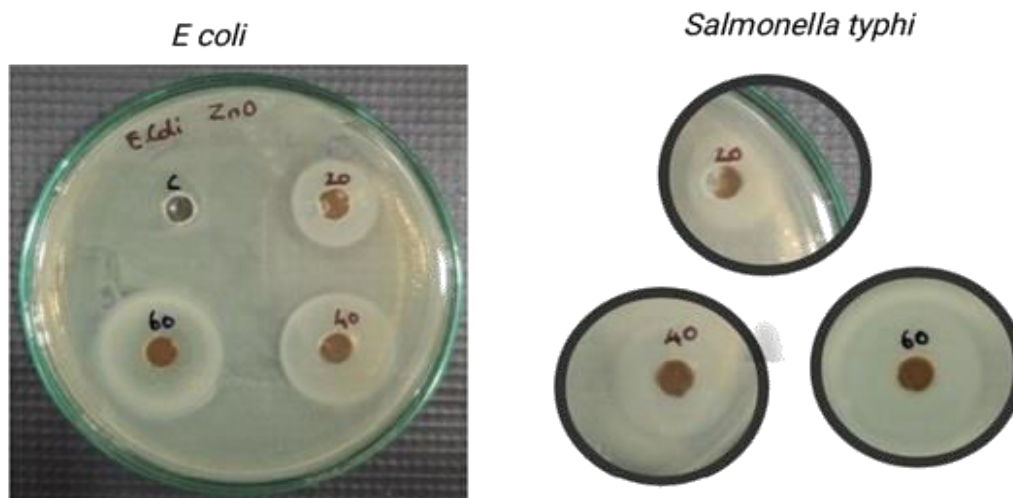


Fig. 5: The zone of inhibition for the E.coli and S.typhi

4. CONCLUSION

It is well known that green synthesis of ZnO-NPs is significantly safer and more eco-friendly than chemical synthesis. In the present investigation, we have described the green synthesis of ZnO-NPs by using *Solanum Nigrum* as capping agent. The functionalization of ZnO particles through *Solanum Nigrum* leaf extract mediated bioreduction of ZnO was investigated by XRD, FTIR, UV-Vis DRS and antibacterial activities. The XRD patterns confirm the formation of ZnO-NPs using *Solanum Nigrum* leaf extract. The diffraction peaks fit well with the hexagonal wurtzite structure of ZnO-NPs. The average particle size of produced ZnO-NPs was determined to be 27.6 nm. The stretching and interactions were investigated using FT-IR spectroscopy. According to UV-Vis absorption study, the sample has a clear and strongly observed absorption edge positioned at 342 nm, indicating a red shift in the UV region. The bandgap value was determined as 3.63 eV. Antibacterial activity was observed in the plate treated with ZnO-NPs. Clear zone of inhibition was noted in *E.coli* and *S.typhi* plates at all the concentrations viz 20ul, 40ul, 60ul respectively. Notably, *E.coli* is highly susceptible for ZnO Nanoparticle compared to *S.typhi*. According to the obtained results the ZnO-NPs inhibit the growth of both normal as well as pathogenic bacterium and hence might be used for coating surgical equipments for aseptic operations in the medical field.

Conflicts of interest

The authors declare that no funds, grants, or other support were received during the preparation of this manuscript.

5. REFERENCES

1. Debabrata Pal. *J Adv Sci Res*, 2023; **14**:86-91.
2. Helen Merina Albert, Lohitha T, Alagarsamy K, et al. *Mat Today Proceed*, 2021; **47**:1030-1034.
3. Saripalli Padmavathi, Chippada Satya Anuradha. *J Adv Sci Res*, 2022; **13**:01-06.
4. Karthick Kannan, Devi Radhika, Kishor Kumar S, et al. *Adv Coll Inter Sci*, 2020; **281**: 102178.
5. Sang Hun Lee, Bong-Hyun Jun. *Int J Mol Sci*, 2019, **20**, 865.
6. Khan MAM, Khan W, Ahamed M, et al. *Sci Rep*, 2017; **7**:12560.
7. Muqsit Pirzada, Zeynep Altintas. *Sensors*, 2019; **19**:5311.
8. Augustine D, Terna, Elias E, et al. *Mater Sci Engg B*, 2021; **272**:115363.
9. Vidhya E, Vijayakumar, S, Prathipkumar S, et al. *Gen Rept*, 2020; **20**:100688.
10. Rajni Verma, Saurabh Pathak, Avanish Kumar Srivastava, et al. *J Alloy Comp*, 2021; **876**: 160175.
11. Zheng ZQ, Yao JD, Wang B, et al. *Sci. Rep*, 2015; **5**:1107.
12. Yedurkar S, Maurya C, Mahanwar P. *Open J Synth Theor Appl*, 2016; **5**:1.
13. Arunkumar S, Karthikeyan E, Rajasekaran R. *J Adv Sci Res*, 2020; **11(3 Suppl7)**:331-334.
14. Ashwini J, Aswathy TR, Achuthsankar, et al. *Biochem Biophys Rep*, 2021; **26**:100995.
15. Chikkanna MM, Neelagund SE, Rajashekarappa KK. *SN Appl Sci*, 2019; **1**:117.
16. Aneta Salayová, Zdenka Bedlovičová, Nina Daneu, et al. *Nanomater*, 2021; **11**: 1005.
17. Menazea AA, Ismail AM, Samy A. *J Inorg Organomet Polym*, 2021; **31**:4250-4259.
18. Samaneh MES, Sharareh M, Babak F et al. *Bull Mater Sci*, 2021; **44**:129.
19. Akl MA, Nidá MS, Marwa MA, et al. *Chem Internat*, 2020; **6**: 42-48.
20. Helen Merina Albert, Alosious Gonsago C, *J Electron Mater*, 2022; **51**:4555-4564.
21. Singh SJ, Lim YY, Hmar JJJL, et al. *Appl Phys A*, 2022; **128**:188.
22. Anindita De, Riya Das, Preeti Jain, et al. *Mater Today Proceed*, 2022; **49**:3122-3125.
23. Albert HM, Joseph APA, Bhagavannarayana G, et al. *J Therm Anal Calorim*, 2014; **118**:333-338.
24. Khan MM, Harunsani MH, Tan AL, et al. *Bioprocess Biosyst Eng*, 2020; **43**:1499-1508.
25. Bruna Lallo da Silva, Bruno Leonardo Caetano, Bruna Galdorfini Chiari-Andréo, et al. *Coll Surf B Biointer*, 2019; **177**:440-447.